

ANALYSIS OF LOADS AND STRESSES IN STRUCTURAL ELEMENTS OF HOISTING INSTALLATIONS IN MINES

S. W o l n y, F. M a t a c h o w s k i

AGH University of Science and Technology
Faculty of Mechanical Engineering and Robotics

Al. Mickiewicza 30, 30-059 Kraków, Poland

Shaft steelwork-conveyance interactions are present in the literature on the subject available in Poland, these problems have been extensively studied by the research teams from AGH-UST, the Central Mining Institute and the Silesian University of Technology. Despite novel and original solutions in this field, fresh problems tend to appear which have to be solved promptly. In this context an attempt to determine the force of steelwork-conveyance interaction due to irregularities of the guiding string might prove useful in the strength analysis of the conveyance or the shaft steelwork.

This study attempts to determine the steelwork-conveyance interaction force and carrying elements stresses based on the dynamic analysis of the hoist operation, taking into account the irregularities or misalignment of the guiding string and their random occurrence. To validate the model some experiment on a real object were done.

Key words: mine hoists, dynamics, loading.

1. INTRODUCTION

Conveyances have to be transferred to the shaft landing for the purpose of loading or unloading. This is made possible by the headframe structure which supports the head-gear pulleys and, in some cases, also the winder machine.

The headframe design is chosen depending on the projected functions of the hoist and the shaft, and of the shaft location on the surface. We can have braced structures or hoist towers where the hoists are located in the head gear. The schematic diagram of a hoisting installation with the winder machine placed in a hoist tower is shown in Fig. 1a. Figure 1b shows the schematic diagram of a hoisting installation with the winder installed on the shaft landing.

Nowadays the majority of towered head gears are erected to handle multiple rope hoisting installations only. Apart from the winder mechanisms, their house driving wheels, ventilators, rectifiers or converters. The head structure is also required, to accommodate the guiding systems, fender beams and jack catch devices. Since the multiple-rope towered hoists with pulley blocks have now

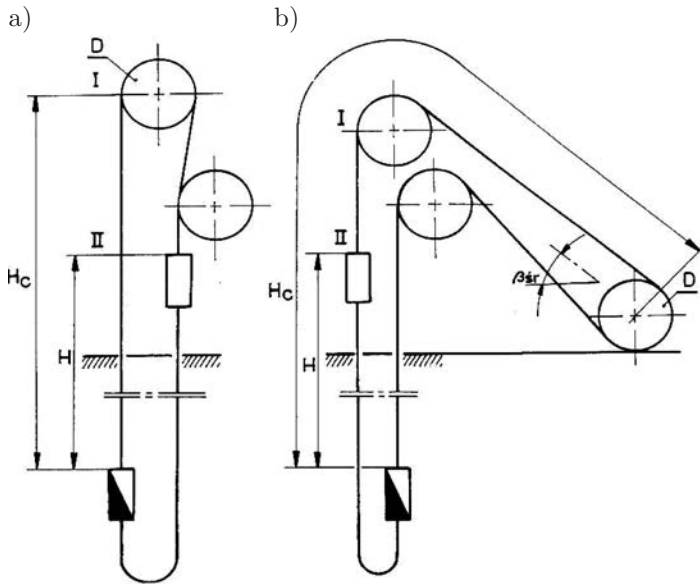


FIG. 1. Schematic diagram of a multiple rope hoisting installation: a) winder in the hoist tower; b) winder on the brink of the shaft.

become the most widespread, this work will be restricted to hoisting installations most popular in our conditions, shown schematically in Fig. 2.

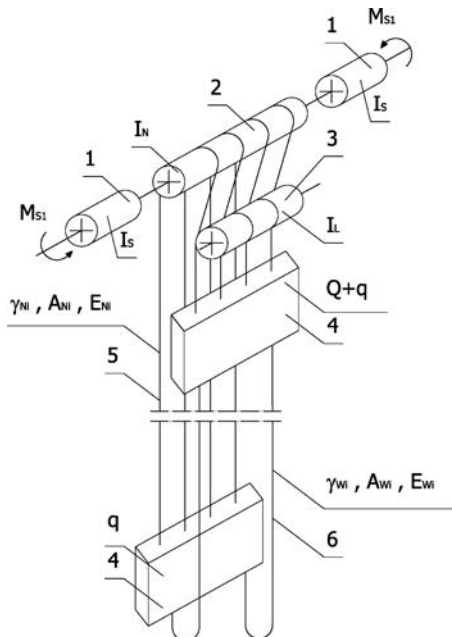


FIG. 2. Schematic diagram of the hoisting installation.

The components of the hoisting installation include:

- 1 – low-torque dc motors, the inertia moment of their armature being I_s ;
- 2 – multiple rope Koepe pulley of diameter D and inertia moment I_N ;
- 3 – deflecting pulleys of the inertia moment I_L ;
- 4 – skips (conveyances) of the mass q and loading capacity Q , the upper skip being loaded;
- 5 – branches of hoisting ropes arranged in parallel, of the rope density γ_N and stiffness under tension $A_N E_N$;
- 6 – branches of tail ropes arranged in parallel, of the rope density γ_W and stiffness under tension $A_W E_W$.

Normative standards [1–3] to be applied when designing structural elements of a conveyance (item 4 in the hoist diagram, see Fig. 2) take into account the vertical loads only (loads due to the suspension systems and the tail ropes), whilst the rectilinear vertical motion of the conveyance is disturbed by unevenness of the guide column along which the guide rollers, attached to the conveyance, have to slide. This unevenness (or guide misalignment) gives rise to horizontal forces: the forces of conveyance-shaft steelwork interactions, which are responsible for damaging of the strings connecting the structural components of the conveyance (head, skip hopper, lower frame). So far, many attempts [4–6, 9] have been made to determine those forces, yet the results are still far from satisfactory. In other words, we still lack theoretical relationships defining their value, verified by experiments done on a real object. The authors made a great effort to address this problem, basing on numerical analysis of the FEM model and the results of experiments done on a real object in a colliery in Poland. Furthermore, the authors investigated the state of stress in strings connecting the structural components of the conveyance.

2. CONVEYANCE MODEL (FEM 3D)

The numerical model of the conveyance (FEM 3D) was developed, *inter alia*, to find the interaction forces between the conveyance and shaft steelwork and to determine the state of stress and strain in selected elements of the conveyance.

Numerical models of conveyances (FEM 3D) of the lifting capacity 17 Mg (Fig. 3) are based on the technical data of real mine shaft conveyances operated in a colliery in Poland, where the guide misalignment is measured, too.

The numerical model of the conveyance is a beam and surface model, incorporating the following elements (Fig. 4):

- head structure modelled with beam elements;
- skip hopper modelled by beam elements (hopper frame) and by surface elements (hopper panelling);

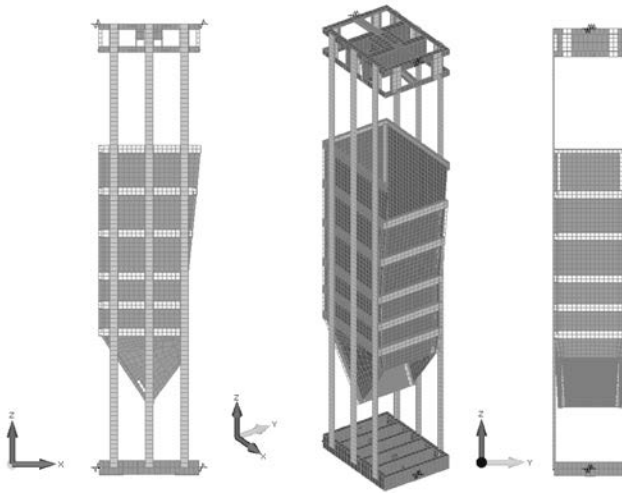


FIG. 3. Numerical (FEM) model of a skip of the lifting capacity 17 Mg.

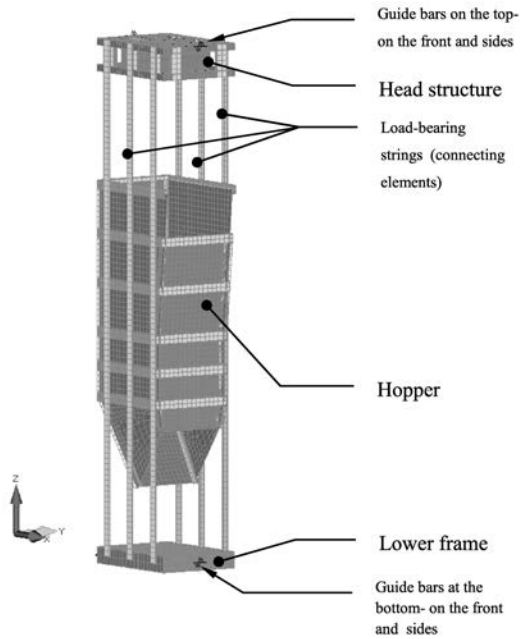


FIG. 4. Structural elements of the skip considered in the FEM model.

- lower frame modelled by beam elements (likewise the head structure);
- load-bearing strings, connecting those three structural components, modelled as beams;
- front and lateral guide bars modelled as elastic-damping elements.

The numerical model (Fig. 4) captures the operating conditions of the mine shaft conveyance. In the vertical direction, the model is supported on the head structure (conveyance suspension) at the attachment point of the hoisting rope thimble (Fig. 5), and at the point where tail ropes (Fig. 6) are attached to the lower frame (tail rope suspension), the time-variant force is applied equivalent to the instantaneous skip loading, due to the weight of tail ropes.



FIG. 5. Attachment of tail ropes for the skip with the support point in the FEM model revealed (red ring).



FIG. 6. Bottom guide bar assembly and attachment of tail ropes.

At the point where the conveyance interacts with the shaft steelwork, the model is supported in the lateral (horizontal) direction via the roller guides systems (on the front and on the sides) by elastic-damping elements, their elasticity and damping factor being equal to relevant elasticity and damping coefficients of the guide bar systems on the front and on the sides (Fig. 7).



FIG. 7. Top guide bar assembly for the skip.

Horizontal displacements of the system during the conveyance travel up and down at the fixed speed v , are induced by misalignment (irregularities) of the guide column $x(t)$, obtained by measurements taken on a real plant. These irregularities impact on the guide bars at the front and on the sides. For the skip travel at the fixed speed v , it is assumed that the function governing the displacements of the lower guide bars, fixed to the bottom frame $x(t+\tau)$, is back-shifted with respect to that governing the displacement of upper guides fixed to the head structure, for the period of time $\tau = l/v$ equal to that required by the conveyance to travel the distance l between the upper and lower guide bars (Fig. 8).

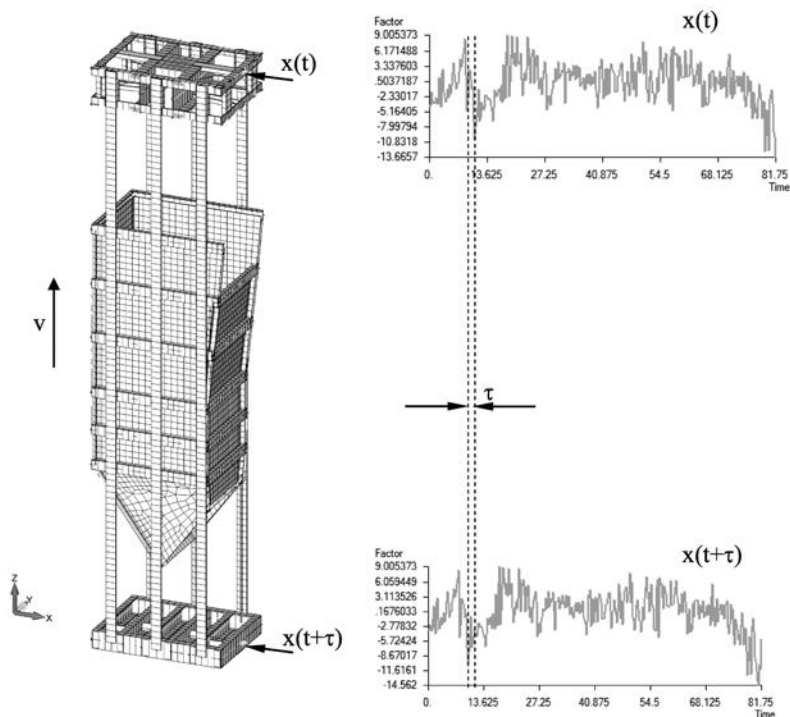


FIG. 8. Schematic diagram of skip loading by the displacement $x(t)$.

In numerical analysis we consider a loaded skip, modelled by mass elements (invisible in model diagrams).

2.1. Strength analysis

The numerical model of a conveyance is further utilized in the endurance analysis (the state of stress and strain) in structural elements of the system during the full hoisting cycle (loading, hoisting up from the shaft bottom, steady ride, reaching the top station, unloading, ride down of an empty skip). The endurance analysis would yield the conveyance-shaft steelwork interaction forces acting during the conveyance ride at the speed v . Spectral densities of those forces, are obtained, too.

Figure 9 shows a plot of the conveyance-shaft steelwork interaction forces in the system comprising upper and lower front guide bars (Fig. 10). Plots of conveyance-shaft steelwork interaction forces reveal the maximal values of these forces and their amplitudes. Figure 11 shows the plots of spectral densities of conveyance-shaft steelwork interaction forces (for three hoisting velocities $v = 12, 16, 20$ m/s), based on the results of the dynamic analysis of the FEM model (FEM 3D).

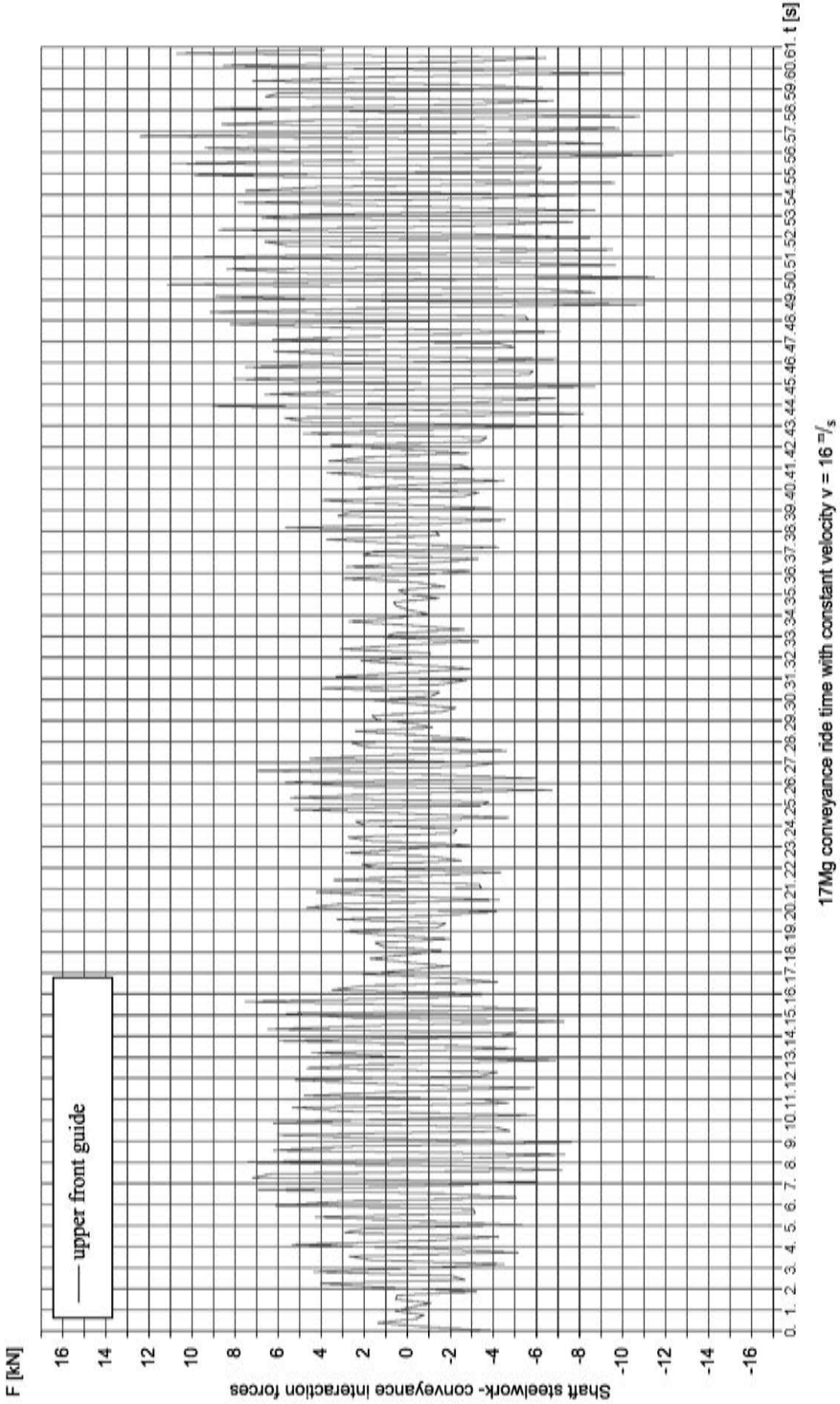


FIG. 9. Shaft steelwork-conveyance interaction forces in the system of upper front guides.

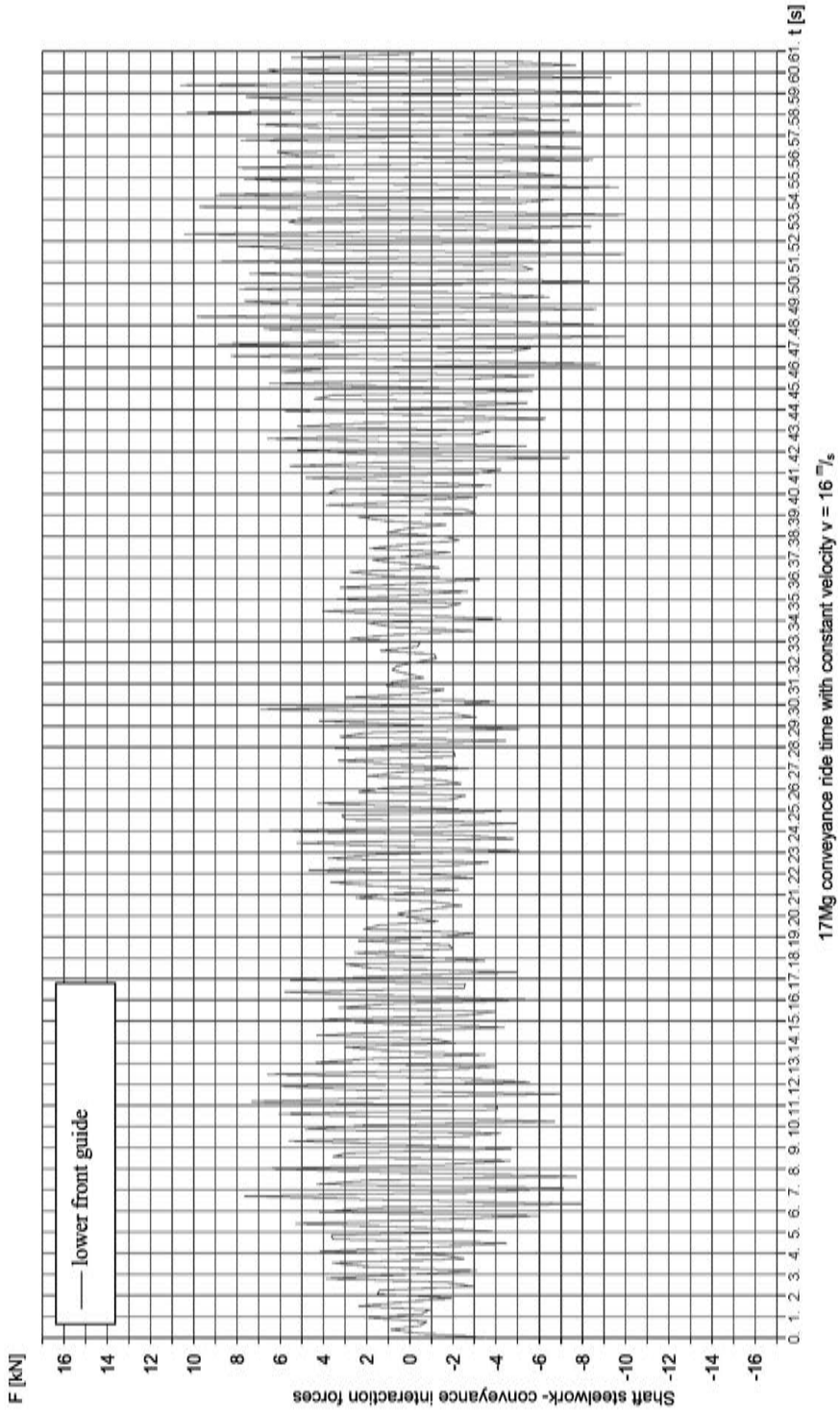


FIG. 10. Shaft steelwork-conveyance interaction forces in the system of lower front guides.

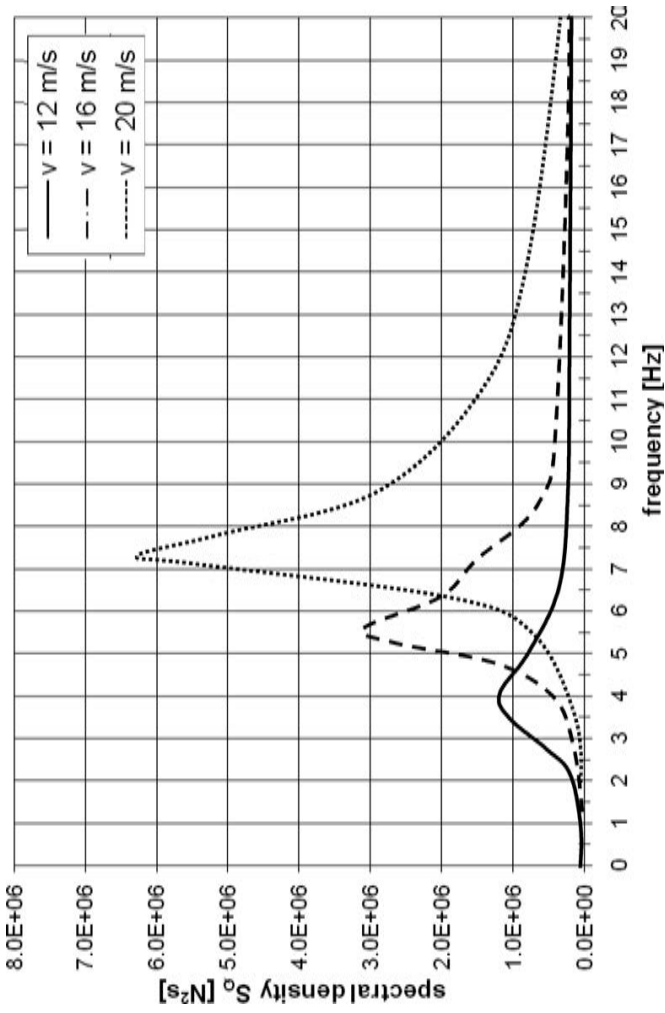


FIG. 11. Spectral densities of conveyance-shaft steelwork interaction forces obtained from solving of the 3D FEM model.

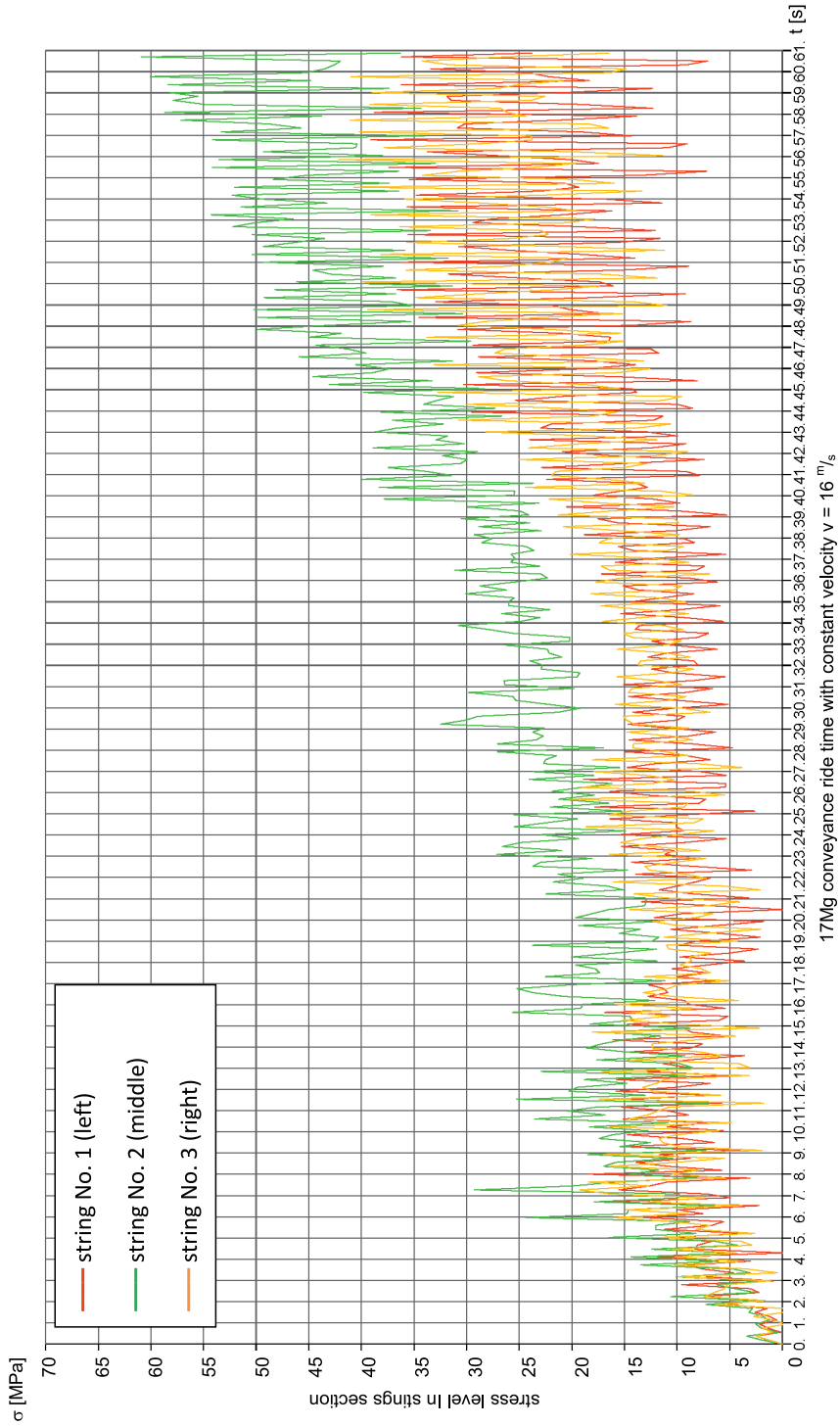


FIG. 12. Normal stresses in string cross-section at the attachment point to the head structure.

Furthermore, the endurance analysis reveals the state of stress in structural elements of the conveyance while it is hoisted from the loading station at the shaft bottom. Figure 12 shows the plots of stresses in cross-sections of strings at their attachment points to the head structure, for the steady ride $v = 16$ m/s, when the loaded conveyance is hoisted up from the loading station at the bottom.

3. EXPERIMENTS ON A REAL OBJECT

Roller guides (Fig. 13) in hoisting installations are used to guide a conveyance along the vertical guides in the shaft. Therefore they have to transmit the conveyance-shaft steelwork interaction forces. Deformation of elastic elements of the roller guide might be used to determine the extent of this interaction.



FIG. 13. Roller guide assembly- at the bottom.

Figure 14 shows the schematic diagrams of the front roller guide mechanism (Fig. 14a) and of the lateral guide (Fig. 14b), being the elements of the tested hoist. To determine the shaft steelwork-conveyance interaction forces, we recall the procedure of measuring of the displacement X_2 (displacement of the roller housing with respect to the guide bar, permanently fixed to the head structure, lower frame) of the conveyance (Fig. 14).

The formula governing the load acting upon the front and lateral roller guide system, as a function of its displacement X_2 and the displacement X_2 is derived, basing on laboratory data for various types of guide bar systems summarized in the papers [7].

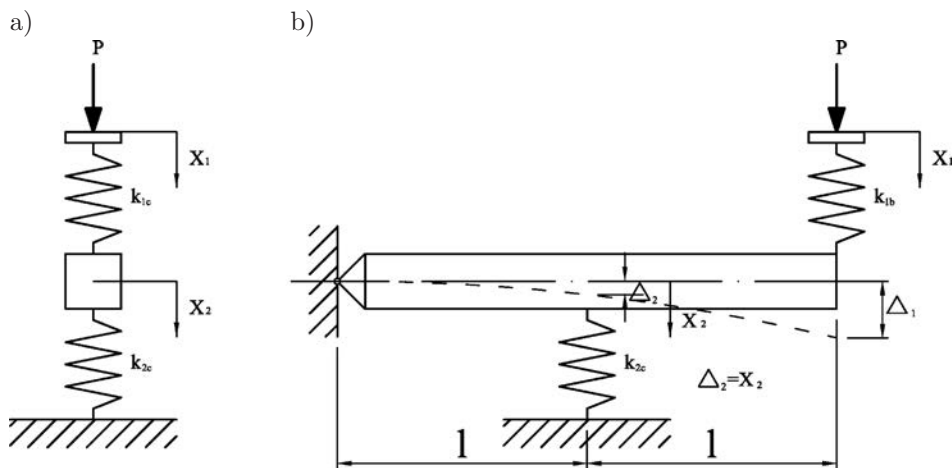
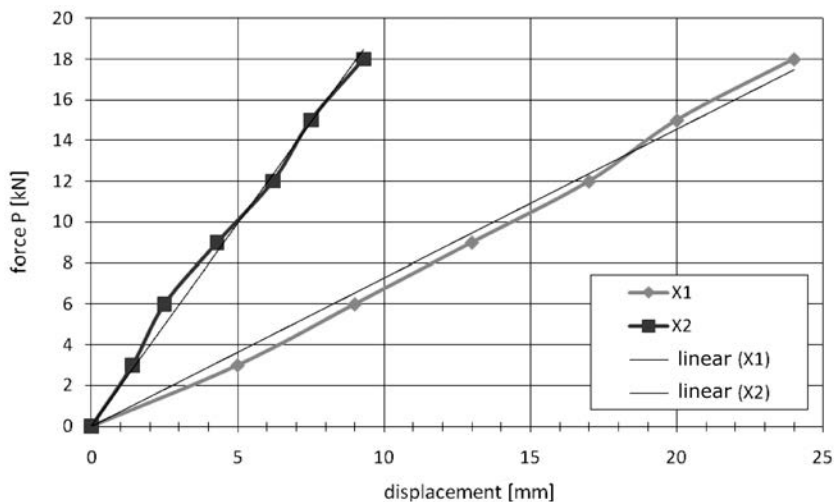


FIG. 14. Diagrams of the roller guide systems: a) front; b) lateral.

Figure 15 shows the static characteristic of the front roller guide (loading force P vs. the total displacement X_1 , the displacement X_2 being simultaneously registered). The static characteristic of the lateral guide is given in Fig. 16. In both cases, the indicated linearized characteristics $P(X_1)$ and $P(X_2)$ agree well with those obtained experimentally.

Measurements of displacement (X_2 in Fig. 15a) were taken with induction sensor and strain gauges attached to the measuring beam, in a device fabricated especially for the purpose of the research program [7].

FIG. 15. Static characteristic of the front roller guide obtained by measurements (X_1 – total displacement; X_2 – displacement of the roller housing) and its linearized form.

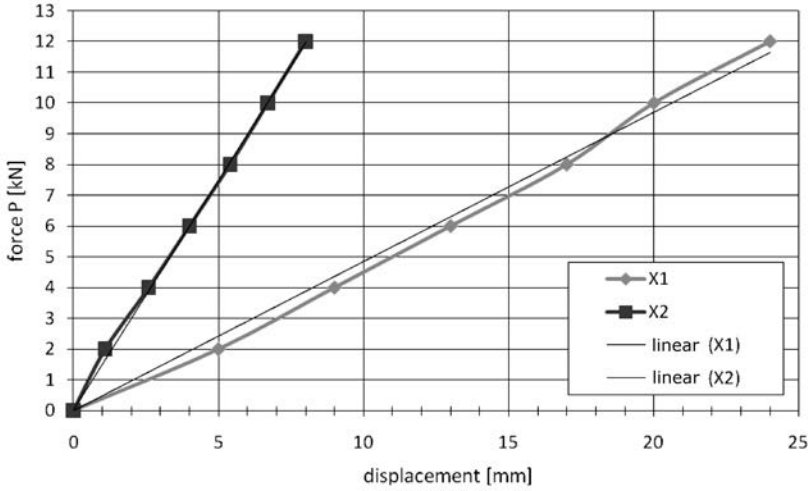


FIG. 16. Static characteristic of the lateral roller guide obtained by measurements (X_1 – total displacement; X_2 – displacement of the roller housing) and its linearized form.

The data obtained from periodic overhauls of skips and cages operated in Polish mines indicate that a majority of the reported conveyance failures are caused by fatigue cracking [6]. These cracks appear and propagate mostly in load-bearing strings or in welded sections, in the areas where they are attached to the conveyance structure. In order to find the real value of stress in the areas where fatigue cracks are registered, measurements are taken with strain gauges in the service conditions.

Measurements of the conveyance-shaft steelwork interaction force are taken for the hoisting installation, in which the guide misalignment was measured (lifting capacity $Q = 17$ Mg, hoisting distance $H = 1020$ m, hoisting speed 16 m/s).

The measurements covered a full cycle of skip operations:

1. Ride down to the charging station (on the shaft bottom);
2. Loading (17 Mg);
3. Hoisting of a loaded skip to the shaft top;
4. Unloading at the shaft top.

Measurements were taken during three consecutive full cycles of skip operation. Figure 17 shows the arrangement of measuring sensors and numbering of relevant guide bars. Measurements covering the full cycle of skip operations were repeated three times. Figure 18 shows the strain gauge fixed to the upper front roller guide and Fig. 19 shows the induction sensors attached to the lower guide assembly. Figure 20 shows the plots of measured displacements of the guiding elements in the front roller guide.

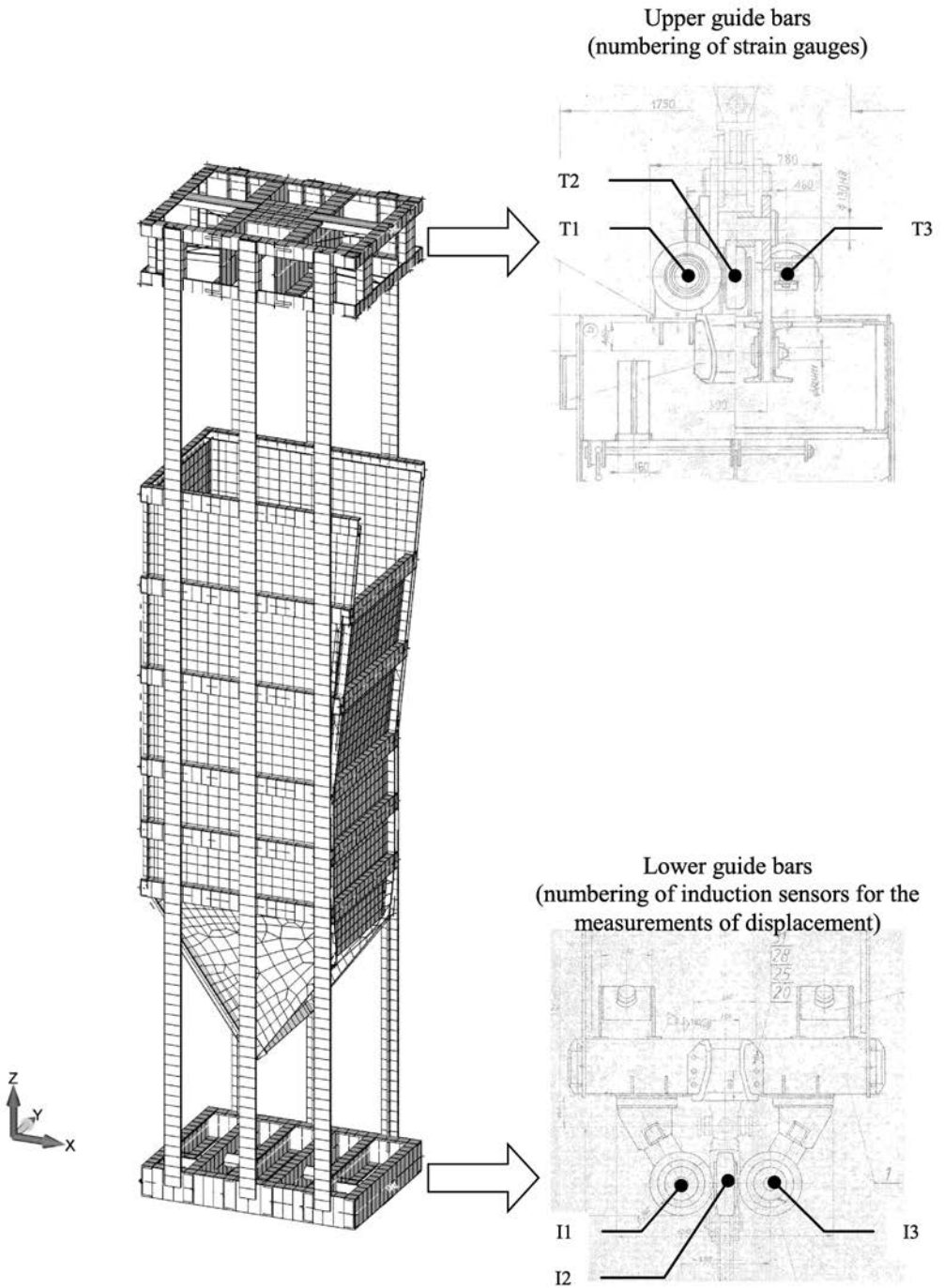


FIG. 17. Configuration and numbering of measurement points.

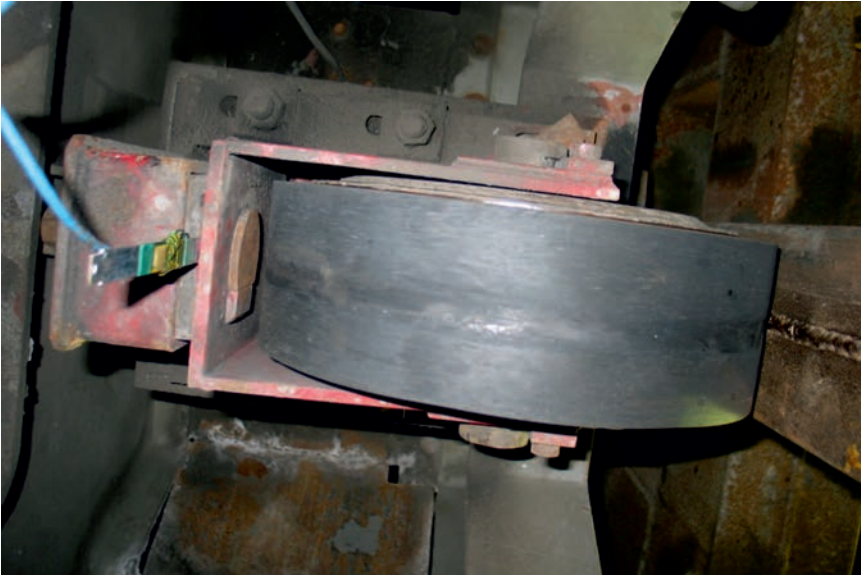


FIG. 18. Upper front guide with an attached strain gauge, general view.



FIG. 19. Lower roller guide assembly with the attached induction sensors.

Measured displacements in the conveyance guiding system in conjunction with the roller guide characteristic (Figs. 15, 16), yield the maximal shaft steel-work-conveyance interaction forces in the system comprising front roller guides on the top (fixed to the head structure) and at the bottom (fixed to the lower frame). The results are compiled in Table 1.

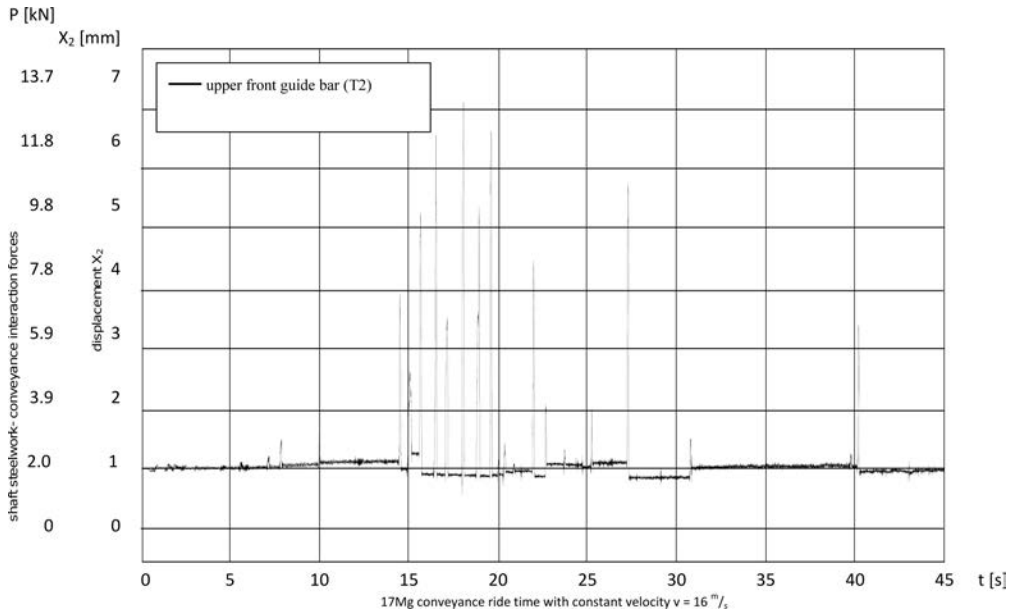


FIG. 20. Registered displacement X_2 of the upper front guide bar (Travel I) during the ride up of a loaded conveyance.

Table 1. Maximal shaft steelwork-conveyance interaction forces.

Cycle	Phase	Upper roller guide assembly			Bottom roller guide assembly		
		Side left P_{bl} [kN]	Front P_c [kN]	Side right P_{br} [kN]	Side left P_{bl} [kN]	Front P_c [kN]	Side right P_{br} [kN]
I	Ride down (empty)	1.7	2.4	1.6	2.0	0.8	0.2
	Loading	1.4	2.0	2.2	1.0	0.2	0.1
	Ride up (loaded)	3.4	12.8	9.2	1.7	9.0	0.6
	Unloading	0.2	0.8	0.4	0.2	0.2	0.4
II	Ride down (empty)	0.6	2.6	6.0	2.2	1.0	0.5
	Loading	0.8	1.0	0.8	0.4	0.4	0.5
	Ride up (loaded)	4.8	12.0	14.0	2.3	7.6	0.6
	Unloading	0.1	0.4	0.3	0.1	0.4	0.4
III	Ride down (empty)	0.6	1.2	6.0	2.0	0.6	0.4
	Loading	0.9	0.4	0.4	0.4	0.6	0.4
	Ride up (loaded)	4.6	11.8	11.8	2.0	6.6	0.6
	Unloading	0.1	0.4	0.8	0.3	1.0	0.3

Basing on experimental data, the plots of spectral density of maximal shaft steelwork-conveyance interaction forces are obtained for the conveyance travel at the fixed speed $v = 16$ m/s during the test. Figure 21 shows the plots of spectral density of the interaction force S_Q :

- black colour – spectral density of force obtained from solving the FEM model,
- red colour – spectral density of force obtained from measurements on a real object.

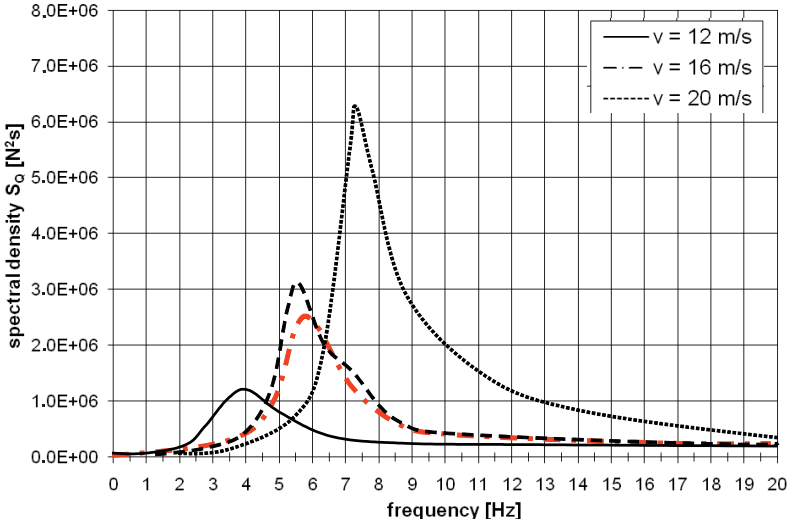


FIG. 21. Spectral densities of “shaft steelwork-conveyance interaction” forces obtained by solving of the 3D FEM model and experimentally (red colour).

Measurements in the load-bearing strings of the conveyance are restricted to stress concentration, revealed by the endurance analysis.

Strain gauges designated as TC1, TC2, TC3, TC4 are attached to the string on the head structure, as shown in Figs. 22 and 23. The sensors TC5, TC6, TC7, TC8 are fixed on the strings beneath the first frame of the hopper (Figs. 24, 25). Sensors TC5 and TC5', TC6 and TC6', TC7 and TC7', TC8 and TC8' are fixed to the opposite surfaces of the strings in the half-bridge configuration and connected to relevant measurement channels. This arrangement allows for measuring of this part of stress which is due to the bending moment acting in the plane perpendicular to that, to which the strain gauges are fixed. Strain gauges are placed at the distance of 135 mm from the lower edge of the frame, and the strain gauge 9 – at the distance of 35 mm from this frame.

Figure 26 shows the stresses measured in the string cross-section throughout the full cycle of skip operation. It is worthwhile to mention that the sensors were attached in the tower structure, at the instant when the loading due to tail ropes should be the greatest. That is why the plot reveals 26 compressive stresses not experienced in real service, registered in the initial phase of the ride down and ride up. Therefore, the whole plot should be shifted ‘upwards’ by the value of the smallest measured stress (as given in Table 2).

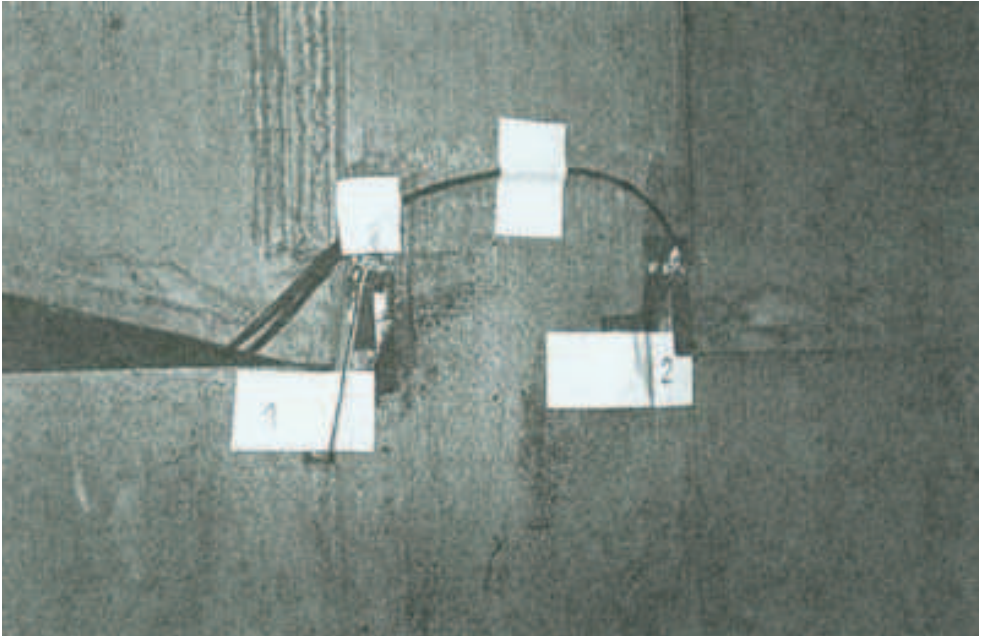


FIG. 22. Strain gauges TC1 and TC2 fixed to the left-side string, at the attachment point to the head structure.



FIG. 23. Strain gauges TC3 and TC4 fixed to the mid-point string, at the attachment point to the head structure.



FIG. 24. Sensors TC5, TC5', TC6, TC6' fixed at the point where the mid-point string is connected with the hopper structure.

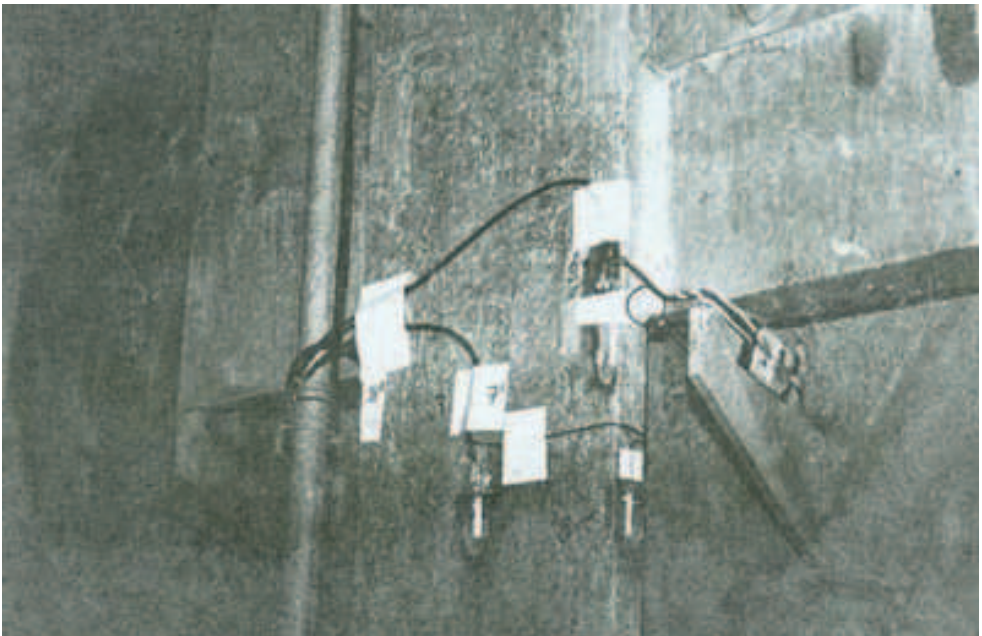


FIG. 25. Sensors TC7, TC7', TC8, TC8' and TC9, fixed at the point where left-side string is connected with the hopper structure.

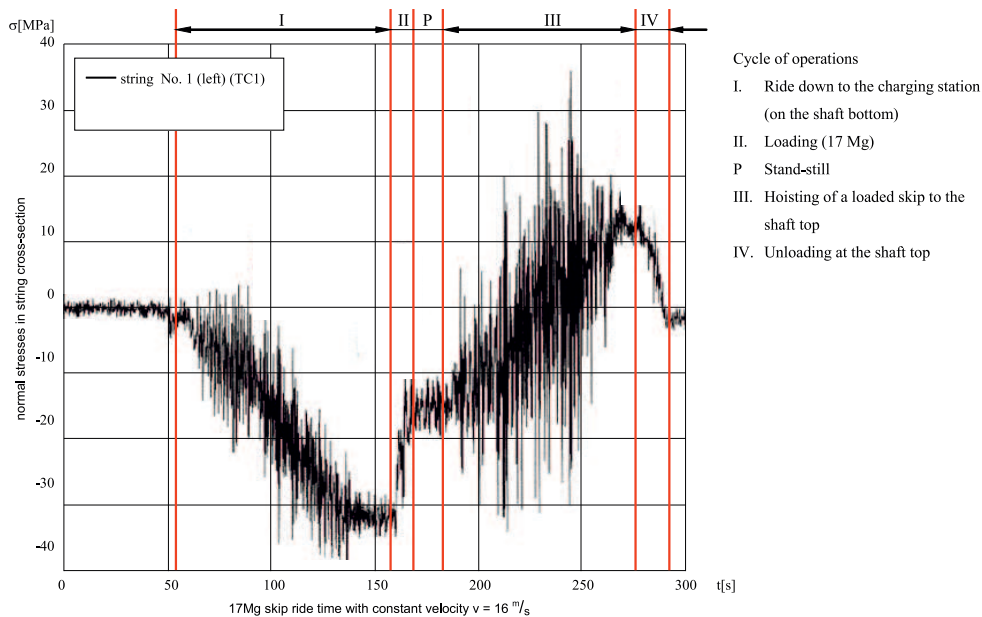


FIG. 26. Stress in the string cross-section registered by the sensor TC1.

The maximal stresses and their amplitudes are compiled in Table 2 for each cycle of operation, and compared with the FEM model solutions.

Table 2. Maximal stresses and their amplitudes in string cross-sections obtained experimentally, for the ride up of the loaded conveyance at the speed $v = 16$ m/s.

Cycle	Left-side string				Middle string			
	Attachment point to the skip head structure TC1, TC2		Attachment point to the hopper frame TC7, TC8, TC9		Attachment point to the skip head structure TC1, TC2		Attachment point to the hopper frame TC7, TC8, TC9	
	max. [MPa]	ampl. [MPa]	max. [MPa]	ampl. [MPa]	max. [MPa]	ampl. [MPa]	max. [MPa]	ampl. [MPa]
I	68	45	75	43	62	38	71	41
II	69	43	79	44	63	38	72	42
III	68	46	76	43	61	38	71	42
MES	43	22	45	26	62	43	63	43

4. CONCLUSIONS

The shaft steelwork-conveyance interaction forces and stresses, measured in strings connecting the structural elements of the conveyance, agree well with numerical FEM solutions (3D FEM model).

Stresses are measured in load-bearing strings; the extreme and the middle ones, are very similar, whilst stresses obtained by the FEM analysis (the solution for three strings) would significantly differ. One has to bear in mind, however, that the FEM model was developed basing on the technical specification data of the machine, so it fails to take into account the stress experienced during the assembly procedures and the ‘adjustment’ of the structure to the operating conditions. These factors prove to be major determinants of stress distribution in load-bearing strings.

The analysis of shaft steelwork-conveyance interactions due to misalignment of the guide column and their influence on stresses experienced in structural elements of the conveyance, can become a starting point for defining the fatigue endurance of load-bearing components of the conveyance. Furthermore, this study can be utilised in optimisation of structural parameters of the system (mass, fatigue endurance).

REFERENCES

1. *Regulation of Economy Minister from 28 June 2002 on safety and occupational health* [in Polish], Dz.U. Nr 139, poz. 1169.
2. *Regulation of Economy Minister from 9 June 2006 on safety and occupational health* [in Polish], Dz.U. Nr 124, poz. 863.
3. *Regulation of The Council of Ministers from 30 April 2004 on acceptance of products for use in mining* [in Polish], Katowice, 2006.
4. S. KAWULOK, *Influence of elasticity of mining vessel on its dynamics* [in Polish], Katowice, Biuletyn GIG, **2**, 94, 1987.
5. D. TEJSZERSKA, *Modeling of coupled transverse-longitudinal vibration of mining vessel system* [in Polish], Gliwice: Wyd. Politechniki Śląskiej, 1995.
6. M. PŁACHNO, *Method of measurement and analysis of mining vessel transversal vibration useful to appoint of real vessel and steel works loads* [in Polish], Kraków, Zeszyty Naukowo-Techniczne KTL, **15**, 1999.
7. S. WOLNY, *Dynamic Loading of the Pulley Block In a Hoisting Installation In Normal Operating Conditions*, Archives of Mining Sciences, **54**, 2, 261–284, 2009.
8. S. WOLNY, *Analysis of Loading in the Conveyance – Shaft Steelwork System*, Archives of Mining Sciences, **51**, 4, 529–546, 2006.
9. S. WOLNY, F. MATACHOWSKI, *Operating loads of the shaft steelwork-conveyance system due to random irregularities of the guiding strings*, Archives of Mining Sciences, **55**, 3, 589–603, 2010.